

Article

An Investigation of Quorum Sensing Inhibitors against *Bacillus cereus* in The Endophytic Fungus *Pithomyces sacchari* of the *Laurencia* sp.

Shi-Liang Xiang, Kai-Zhong Xu, Lu-Jun Yin and Ai-Qun Jia * 

Key Laboratory of Tropical Biological Resources of Ministry of Education, School of Pharmaceutical Sciences, Hainan University, Haikou 570228, China

* Correspondence: ajia@hainanu.edu.cn; Tel./Fax: +86-0898-66254967

Abstract: *Bacillus cereus*, a common food-borne pathogen, forms biofilms and generates virulence factors through a quorum sensing (QS) mechanism. In this study, six compounds (dankasterone A, demethylincisterol A₃, zinnimidine, cyclo-(L-Val-L-Pro), cyclo-(L-Ile-L-Pro), and cyclo-(L-Leu-L-Pro)) were isolated from the endophytic fungus *Pithomyces sacchari* of the *Laurencia* sp. in the South China Sea. Among them, demethylincisterol A₃, a sterol derivative, exhibited strong QS inhibitory activity against *B. cereus*. The QS inhibitory activity of demethylincisterol A₃ was evaluated through experiments. The minimum inhibitory concentration (MIC) of demethylincisterol A₃ against *B. cereus* was 6.25 µg/mL. At sub-MIC concentrations, it significantly decreased biofilm formation, hindered mobility, and diminished the production of protease and hemolysin activity. Moreover, RT-qPCR results demonstrated that demethylincisterol A₃ markedly inhibited the expression of QS-related genes (*plcR* and *papR*) in *B. cereus*. The exposure to demethylincisterol A₃ resulted in the downregulation of genes (*comER*, *tasA*, *rpoN*, *sinR*, *codY*, *nheA*, *hblD*, and *cytK*) associated with biofilm formation, mobility, and virulence factors. Hence, demethylincisterol A₃ is a potentially effective compound in the pipeline of innovative antimicrobial therapies.

Keywords: *Laurencia* sp.; endophytic fungus; *Pithomyces sacchari*; demethylincisterol A₃; *Bacillus cereus*; quorum sensing



Citation: Xiang, S.-L.; Xu, K.-Z.; Yin, L.-J.; Jia, A.-Q. An Investigation of Quorum Sensing Inhibitors against *Bacillus cereus* in The Endophytic Fungus *Pithomyces sacchari* of the *Laurencia* sp. *Mar. Drugs* **2024**, *22*, 161. <https://doi.org/10.3390/md22040161>

Academic Editor: Dehai Li

Received: 21 February 2024

Revised: 28 March 2024

Accepted: 29 March 2024

Published: 31 March 2024



Copyright: © 2024 by the authors. Licensee MDPI, Basel, Switzerland. This article is an open access article distributed under the terms and conditions of the Creative Commons Attribution (CC BY) license (<https://creativecommons.org/licenses/by/4.0/>).

1. Introduction

Seaweeds, the largest group of oceanic plants, are capable of producing various metabolites, including polysaccharides, terpenes, and lectins [1]. Algal metabolites exhibit a range of beneficial effects, such as antibacterial, antiviral, antioxidant, and anticancer properties [1–4]. Endophytic fungi, residing within the plant body, coexist without harming the host and can synthesize compounds similar to those produced by the host plant [5]. For instance, the fungal endophyte *Taxomyces andreanae*, found within the inner bark of the *Taxus brevifolia* (Pacific yew tree), is capable of synthesizing paclitaxel derivatives [6]. Similarly, *Diaporthe longicolla*, an endophyte from the leaves of *Saraca asoca*, produces metabolites with noted antibacterial and antioxidant properties [7]. The ethyl acetate extract from *Nigrospora sphaerica*, another endophytic fungus, exhibits potent antioxidant activities, effectively combating free radicals [8]. Additionally, *Hyllosticta capitalensis*, an endophyte, is known for generating a variety of bioactive compounds that possess both antibacterial and antitumor potential [9]. Recent studies reveal that bioactive substances from endophytic fungi, known for their antioxidant, antibacterial, anti-inflammatory, and cancer cell inhibitory effects, have become a prominent focus for screening and research [10].

Foodborne diseases stemming from pathogens constitute a widespread global public health concern [11]. *Bacillus cereus* is a Gram-positive bacterium known for its ability to cause food poisoning [12]. Widely distributed in air, water, and soil, *B. cereus* may be present in various foods, including potatoes, rice, and beans [12]. *B. cereus* can produce

enterotoxins and emetic toxins, leading to symptoms such as diarrhea and vomiting in affected individuals [13]. At the same time, it can form biofilms, enhancing its efficiency in producing harmful metabolites [14]. With the assistance of biofilms, *B. cereus* can evade the decomposition of digestive enzymes [15]. The flagella of *B. cereus* aid in movement to suitable locations and the formation of *B. cereus* biofilm is intricately connected to this locomotion process [16]. It can modulate gene expression through quorum sensing (QS), exercising control over biofilm formation, virulence factors, and spore production [17].

Given that the production of harmful toxins, as well as functions like mobility and membrane activity in *B. cereus*, rely on QS, addressing its impact on human health underscores the importance of developing treatments to disrupt its QS. Therefore, this study aimed to identify compounds from marine algal endophytic fungi that can inhibit the QS function of *B. cereus*, thereby attenuating its pathogenicity.

2. Results

2.1. Identification of Active Strains

Mycelium grown on potato dextrose agar (PDA) exhibited a white coloration and adopted a coarse and cotton-like texture. With the progression of growth, the central color could progressively transform to yellow (Figure 1a). The cells of the conidia exhibited microscopic features such as yellow coloration, oval or slightly oval shape, and 3–5 diaphragms (Figure 1b). The spore wall was smooth. The conidia were septate, elongated, and pale brown in color (Figure 1c). The strain was determined as *Pithomyces* by comparing its gene sequences to those in the gene library (Figure S9). The most closely related strain of W2-F1 was *Pithomyces sacchari* (99.00%) (Figure 1d).

2.2. The Elucidation of Compounds

The isolated six compounds were identified using nuclear magnetic resonance (NMR) and mass spectrum (MS) techniques, and their structures were determined by comparing them with the literature data (Figure 2). The NMR and MS spectra of the six compounds are shown in the Supporting Information (Figures S3–S8).

Compound 1 (4.8 mg) was identified as follows. Dankasterone A ($C_{28}H_{40}O_3$, $m/z = 425.3058$ [$M + H$]⁺, cald. for 425.3050) [18]. ¹H-NMR (400 MHz, MeOD) δ 6.16 (s, H-4, 1H), 5.35–5.31 (m, 2H), 2.87 (td, $J = 8.9, 1.5$ Hz, 1H), 2.69–2.60 (m, 2H), 2.60–2.53 (m, 2H), 2.51–2.46 (m, 1H), 2.41–2.39 (m, 1H), 2.38–2.34 (m, 1H), 2.09–1.99 (m, 3H), 1.95–1.84 (m, 3H), 1.78–1.68 (m, 3H), 1.56–1.38 (m, 2H), 1.29 (s, H-19, 3H), 1.13 (d, $J = 7.1$ Hz, H-21, 3H), 0.99 (s, H-18, 3H), 0.94 (d, $J = 6.8$ Hz, H-27, 3H), 0.86 (d, $J = 6.7$ Hz, H-26, 3H), 0.84 (d, $J = 6.8$ Hz, H-28, 3H). ¹³C-NMR (101 MHz, MeOD) δ 217.53 (q, C-14), 202.21 (q, C-6), 201.68 (q, C-3), 159.33 (q, C-5), 136.00 (CH, C-23), 134.28 (CH, C-22), 126.55 (CH, C-4), 64.05^a (q, C-8), 55.68^a (q, C-13), 50.96 (CH, C-9), 49.50 (CH, C-17), 44.70 (CH, C-24), 41.42 (CH₂, C-7), 39.96 (CH₂, C-1), 38.99 (CH₂, C-12), 38.63 (CH₂, C-15), 38.49 (CH, C-20), 37.39 (q, C-10), 35.17 (CH₂, C-2), 34.37 (CH, C-25), 25.91 (CH₂, C-11), 24.74 (CH₃, C-19), 24.18 (CH₃, C-21), 24.09 (CH₂, C-16), 20.55 (CH₃, C-27), 20.14 (CH₃, C-26), 18.10 (CH₃, C-28), 17.35 (CH₃, C-18) (^a assignments could be switched).

Compound 2 (8.7 mg) was identified as follows. Demethylincisterol A₃ ($C_{21}H_{32}O_3$, $m/z = 331.2271$ [$M - H$]⁻, cald. for 331.2279) [19,20]. ¹H-NMR (400 MHz, CDCl₃) δ 5.61 (d, $J = 4.2$ Hz, H-2, 1H), 5.25 (dd, $J = 15.2, 7.5$ Hz, H-16, 1H), 5.16 (dd, $J = 15.3, 8.2$ Hz, H-15, 1H), 2.68–2.61 (m, H-8, 1H), 2.33–2.26 (m, 1H), 2.06–2.00 (m, 1H), 1.99–1.94 (m, 1H), 1.90–1.80 (m, 3H), 1.71–1.65 (m, 1H), 1.65–1.60 (m, 1H), 1.52–1.42 (m, 4H), 1.03 (d, $J = 6.2$ Hz, H-14, 3H), 0.91 (d, $J = 6.4$ Hz, H-21, 3H), 0.83 (d, $J = 6.7$ Hz, H-19, 3H), 0.82 (d, $J = 6.6$ Hz, H-20, 3H), 0.60 (s, H-12, 3H). ¹³C-NMR (101 MHz, CDCl₃) δ 171.56 (q, C-1), 170.98 (q, C-3), 134.80 (CH, C-15), 132.96 (CH, C-16), 112.29 (CH, C-2), 105.39 (q, C-4), 55.46 (CH, C-11), 50.51 (CH, C-8), 48.98 (q, C-7), 42.96 (CH, C-17), 40.25 (CH, C-13), 35.37 (CH₂, C-5), 35.19 (CH₂, C-6), 33.17 (CH, C-18), 28.99 (CH₂, C-10), 21.50 (CH₂, C-9), 21.13 (CH₃, C-14), 20.09 (CH₃, C-20), 19.78 (CH₃, C-19), 17.73 (CH₃, C-21), 11.88 (CH₃, C-12).

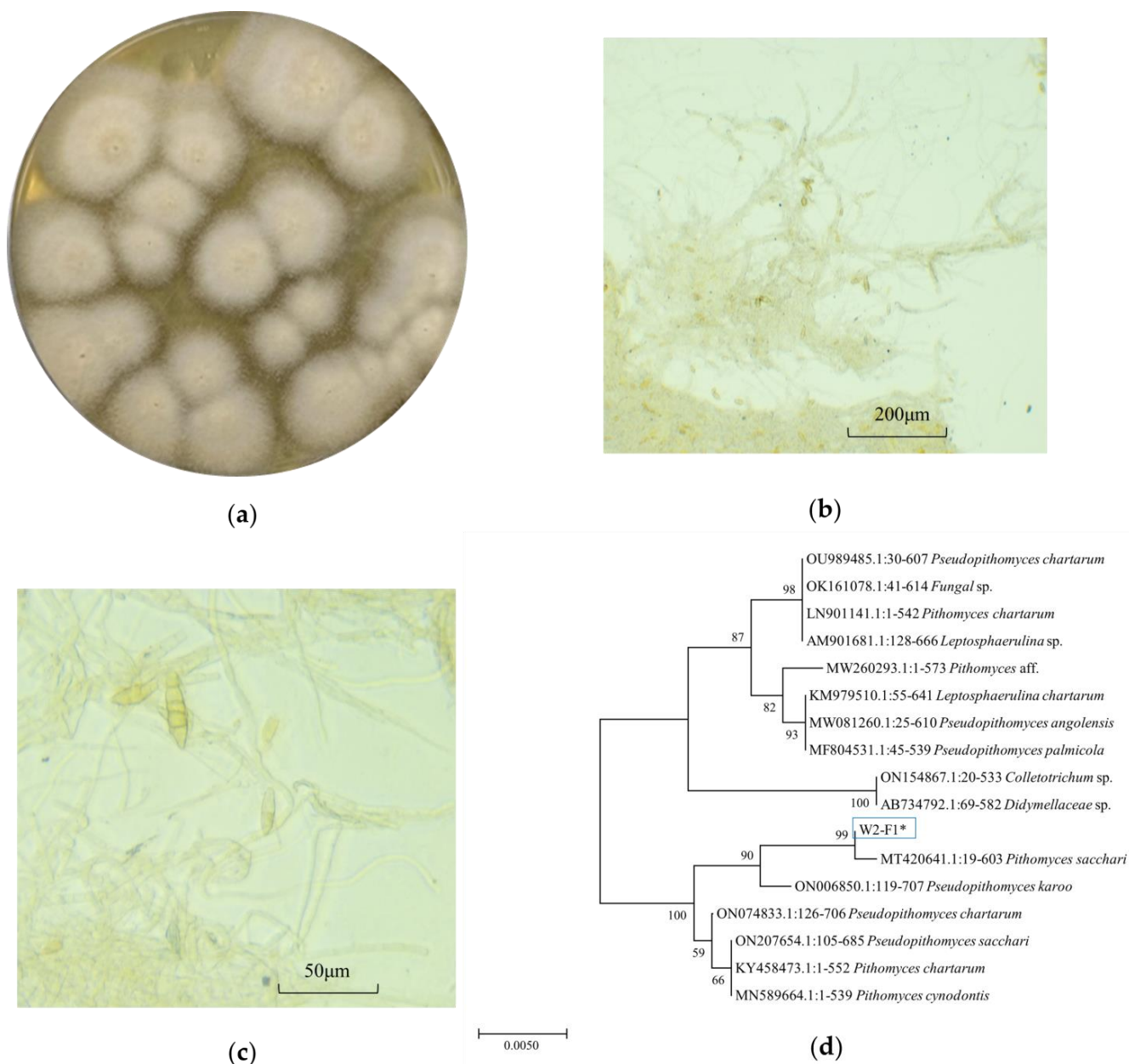


Figure 1. Morphological and phylogenetic tree of *P. sacchari* strain. (a) Colonies grown on a PDA. (b,c) The spores and mycelia were under a microscope with 40× and 100× magnification. (d) Phylogenetic tree.

Compound **3** (3.2 mg) was identified as follows. Zinnimidine ($C_{15}H_{19}NO_3$, $m/z = 262.1435$ [$M + H$] $^+$, cald. for 262.1438) [21]. 1H -NMR (400 MHz, MeOD) δ 7.05 (s, H-6, 1H), 5.49 (t, $J = 6.6$ Hz, H-12, 1H), 4.60 (d, $J = 6.1$ Hz, H-11, 2H), 4.50 (s, H-8, 2H), 3.89 (s, H-9, 3H), 2.16 (s, H-10, 3H), 1.79 (s, H-14, 3H), 1.76 (s, H-15, 3H). ^{13}C -NMR (101 MHz, MeOD) δ 173.70 (q, C-7), 159.86 (q, C-3), 155.15 (q, C-5), 138.94 (q, C-13), 132.43 (q, C-1), 127.47 (q, C-2), 124.43 (q, C-4), 120.93 (CH, C-12), 101.74 (CH, C-6), 66.59 (CH₂, C-11), 60.11 (CH₃, C-9), 45.06 (CH₂, C-8), 25.87 (CH₃, C-14), 18.26 (CH₃, C-15), 9.68 (CH₃, C-10).

Compound **4** (10.8 mg) was identified as follows. Cyclo-(L-Val-L-Pro) ($C_{10}H_{16}N_2O_2$, $m/z = 197.1296$ [$M + H$] $^+$, cald. for 197.1285) [22–24]. 1H -NMR (400 MHz, MeOD) δ 4.20 (t, $J = 7.2$ Hz, H-2, 1H), 4.03 (s, H-4, 1H), 3.63–3.45 (m, H-5, 2H), 2.56–2.42 (m, 1H), 2.39–2.20 (m, 1H), 2.07–1.82 (m, 3H), 1.09 (d, $J = 7.3$ Hz, H-9, 3H), 0.93 (d, $J = 6.9$ Hz, H-10, 3H). ^{13}C -NMR (101 MHz, MeOD) δ 172.60 (q, C-3), 167.57 (q, C-1), 61.51 (CH, C-4), 60.03 (CH,

C-2), 46.18 (CH₂, C-5), 29.87 (CH, C-8), 29.52 (CH₂, C-7), 23.25 (CH₂, C-6), 18.85 (CH₃, C-9), 16.65 (CH₃, C-10).

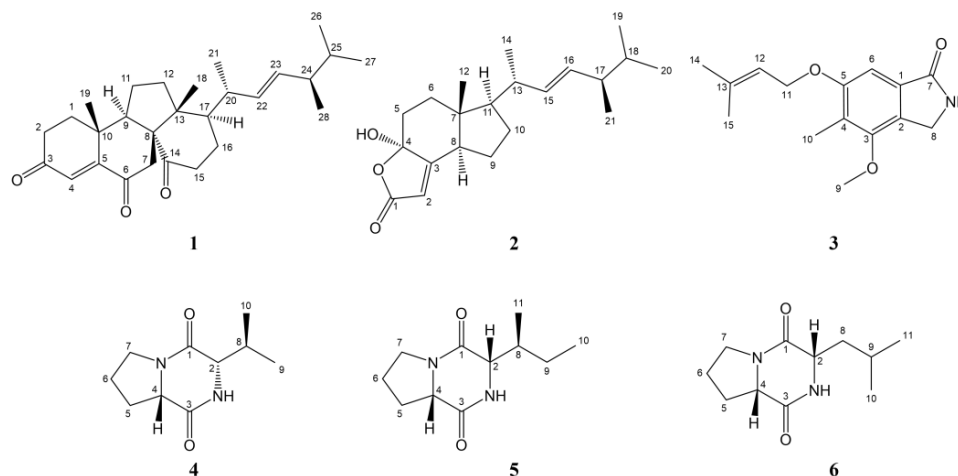


Figure 2. The chemical structures of the isolated six compounds (1–6).

Compound **5** (7.4 mg) was identified as follows. Cyclo-(L-Ile-L-Pro) (C₁₁H₁₈N₂O₂, $m/z = 211.1413$ [M + H]⁺, cald. For 211.1441) [25,26]. ¹H-NMR (400 MHz, MeOD) δ 4.19 (t, $J = 7.0$ Hz, H-2, 1H), 4.07 (s, H-4, 1H), 3.60–3.45 (m, H-5, 2H), 2.36–2.26 (m, H-8, 1H), 2.20–2.12 (m, H-7a, 1H), 2.05–1.98 (m, H-7b, 1H), 1.97–1.87 (m, H-6, 2H), 1.50–1.27 (m, H-9, 2H), 1.06 (d, $J = 7.2$ Hz, H-10, 3H), 0.93 (t, $J = 7.4$ Hz, H-11, 3H). ¹³C-NMR (101 MHz, MeOD) δ 172.45 (q, C-3), 167.59 (q, C-1), 61.30 (CH, C-4), 59.99 (CH, C-2), 46.17 (CH₂, C-5), 37.06 (CH, C-8), 29.54 (CH₂, C-7), 25.41 (CH₂, C-9), 23.22 (CH₂, C-6), 15.52 (CH₃, C-10), 12.57 (CH₃, C-11).

Compound **6** (7.5 mg) was identified as follows. Cyclo-(L-Leu-L-Pro) (C₁₁H₁₈N₂O₂, $m/z = 211.1409$ [M + H]⁺, cald. for 211.1441) [26,27]. ¹H-NMR (400 MHz, MeOD) δ 4.25 (t, $J = 7.1$ Hz, H-2, 1H), 4.12 (dd, $J = 6.8, 3.7$ Hz, H-4, 1H), 3.56–3.44 (m, H-7, 2H), 2.36–2.23 (m, 1H), 2.10–1.78 (m, 5H), 1.58–1.44 (m, 1H), 0.95 (dd, $J = 6.3, 2.5$ Hz, H-10, 11, 6H). ¹³C-NMR (101 MHz, MeOD) δ 172.81 (q, C-3), 168.92 (q, C-1), 60.28 (CH, C-4), 54.63 (CH, C-2), 46.44 (CH₂, C-5), 39.39 (CH₂, C-8), 29.07 (CH₂, C-7), 25.76 (CH, C-9), 23.65 (CH₂, C-6), 23.30 (CH₃, C-10), 22.20 (CH₃, C-11).

2.3. The Growth Profiles of *B. cereus* at Sub-Minimum Inhibitory Concentrations of Demethylincisterol A₃

After quorum sensing inhibitory (QSI)-screening the isolated compounds with *B. cereus*, it was found that only demethylincisterol A₃ had antibacterial and QSI activities. Its minimum inhibitory concentration (MIC) was 6.25 $\mu\text{g/mL}$. At sub-MICs (3.12, 1.56, and 0.78 $\mu\text{g/mL}$), there was no effect on the growth of *B. cereus* (Figure 3).

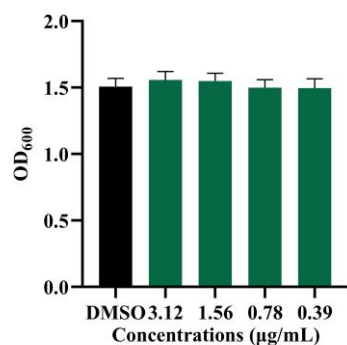


Figure 3. The growth of *B. cereus* at sub-MICs of demethylincisterol A₃. *B. cereus* grew for 24 h in different sub-MICs (3.12, 1.56, and 0.78 $\mu\text{g/mL}$) of demethylincisterol A₃; DMSO was used as the negative control. Error bars represent the standard deviation ($n = 3$).

2.4. Demethylincisterol A₃ Inhibits the Biofilm Formation of *B. cereus*

The results of crystal violet staining indicated a significant reduction in biofilm formation in the demethylincisterol A₃ treatment group when compared to the control group (Figure 4a). When the demethylincisterol A₃ concentration was 3.12, 1.56, and 0.78 µg/mL, the biofilm decreased by 50.2%, 37.9%, and 15.2%, respectively. A substantial reduction in bacterial density after treatment with demethylincisterol A₃ was observed using scanning electron microscopy (SEM) (Figure 4b).

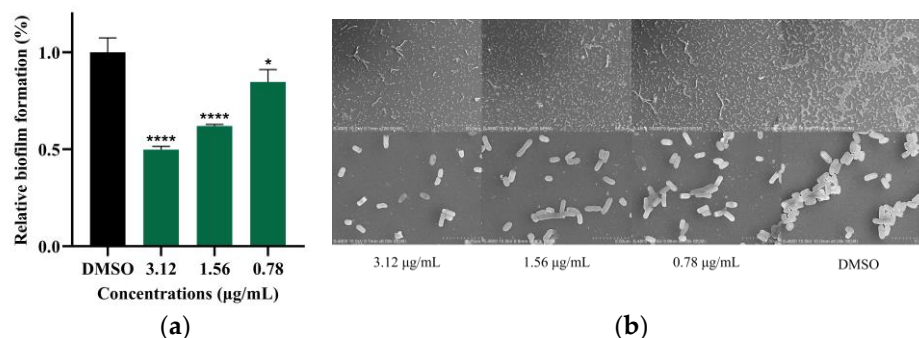


Figure 4. The effect of demethylincisterol A₃ on the biofilm formation of *B. cereus*. *B. cereus* was treated with different concentrations (3.12, 1.56, and 0.78 µg/mL) of demethylsterol A₃ for 24 h, with DMSO as the negative control. (a) Biofilm formation. (b) SEM images of biofilms. Error bars represent the standard deviation ($n = 3$). * $p < 0.05$, **** $p < 0.0001$.

2.5. Demethylincisterol A₃ Inhibits the Swimming of *B. cereus*

The swimming behavior of *B. cereus* was notably hindered after exposure to demethylincisterol A₃ (Figure 5). Under the action of demethylincisterol A₃ at 3.12, 1.56, and 0.78 µg/mL, the swimming ability of *B. cereus* was reduced by 53.9%, 14.7%, and 4.4%, respectively.

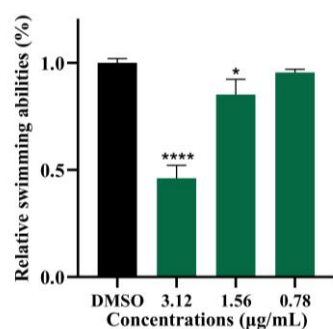


Figure 5. The effect of demethylincisterol A₃ on the swimming of *B. cereus* was examined using a swimming medium. The swimming behavior of *B. cereus* for 24 h of treatment with demethylsterol A₃ at various concentrations (3.12, 1.56, and 0.78 µg/mL) was tested. DMSO served as a negative control. After 24 h of incubation, the swimming diameter was observed and recorded. Values are represented as mean \pm standard deviation ($n = 3$). Significant differences are denoted by * $p < 0.05$ and **** $p < 0.0001$, respectively.

2.6. Demethylincisterol A₃ Inhibits the Protease and Hemolytic Activity of *B. cereus*

After treatment with demethylincisterol A₃, the protease of *B. cereus* was significantly inhibited (Figure 6a). Under the action of demethylincisterol A₃ at 3.12, 1.56, and 0.78 µg/mL, the protease activities of *B. cereus* were reduced by 22.1%, 18.1%, and 10.7%, respectively. The hemolytic activity of *B. cereus* was significantly inhibited when treated with demethylincisterol A₃ (Figure 6b). Under the action of demethylincisterol A₃ at 3.12, 1.56, and 0.78 µg/mL, the hemolytic activities of *B. cereus* were reduced by 15.3%, 11.0%, and 7.6%, respectively.

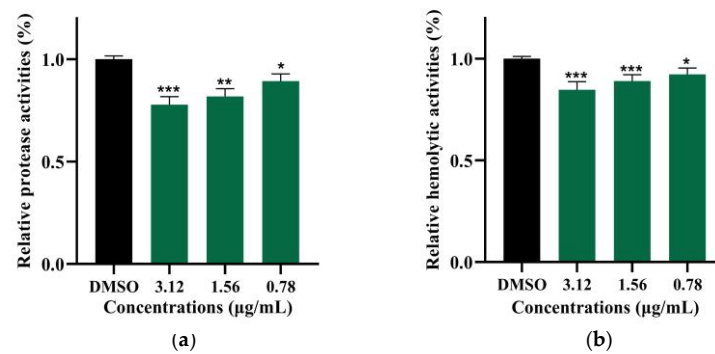


Figure 6. The effect of demethylincisterol A_3 on the virulence factors of *B. cereus*. The virulence factor produced by *B. cereus* after 24 h of treatment with different concentrations (3.12, 1.56, and 0.78 $\mu\text{g/mL}$) of demethylsterol A_3 was evaluated. DMSO was used as a negative control. (a) The protease activity was assessed by examining the clear zone on the skim milk agar plates. (b) The hemolysin activities were analyzed by examining the hemolysis zone on the blood agar plates. Values are represented as mean \pm standard deviation ($n = 3$). Significant differences are denoted by * $p < 0.05$, ** $p < 0.01$, and *** $p < 0.001$, respectively.

2.7. Demethylincisterol A_3 Inhibits the Expression of Key Virulence-Related Genes of *B. cereus*

The expression of virulence-related genes of *B. cereus* was significantly inhibited when treated with demethylincisterol A_3 (Figure 7). Under the action of demethylincisterol A_3 at 3.12 $\mu\text{g/mL}$, the expression of the *sinR*, *tasA*, *papR*, *cytK*, *rpoN*, *hblD*, *comER*, *codY*, *plcR*, and *nheA* genes in *B. cereus* was significantly reduced.

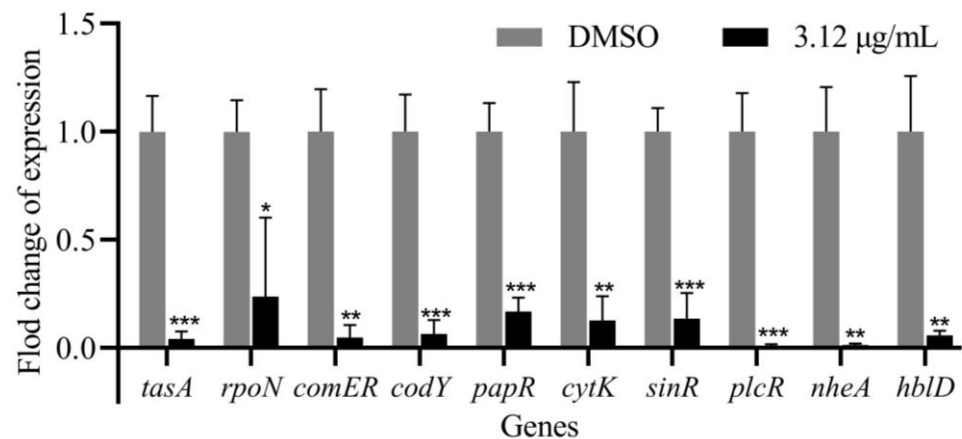


Figure 7. The effect of demethylincisterol A_3 on *B. cereus* gene transcription was investigated. The expression of QS-related genes in *B. cereus* was examined after treatment with 3.12 $\mu\text{g/mL}$ of demethylsterol A_3 for 24 h. DMSO was the negative control. Three biological replicates were conducted and are represented as mean \pm standard deviation ($n = 3$). Significant differences are denoted by * $p < 0.05$, ** $p < 0.01$, and *** $p < 0.001$, respectively.

2.8. Demethylincisterol A_3 Reduces the Mortality Rate of *B. cereus*

As shown in Figure 8, the supernatant of *B. cereus* treated with demethylincisterol A_3 was injected into a *Galleria mellonella* larval model. Only 25% of the larvae in the DMSO group survived after 72 h. However, the survival rate of the experimental group treated with demethylincisterol A_3 was significantly improved, with a survival rate of 88% for the larvae at a concentration of 3.12 $\mu\text{g/mL}$.

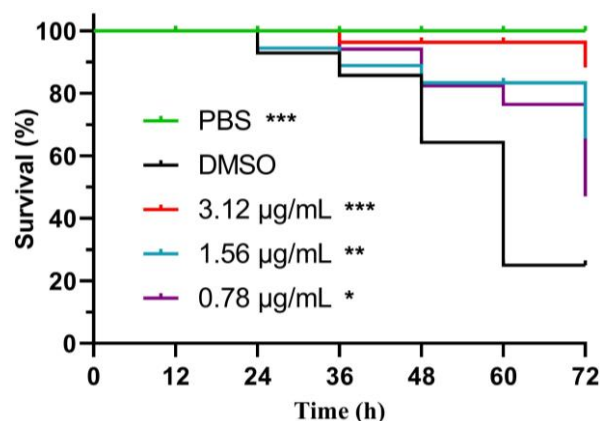


Figure 8. The effect of demethylcisterol A₃ on the survival rate of *G. mellonella* larval models was observed. PBS was the blank control. DMSO was used as a negative control. Statistical analyses were carried out using the log-rank (Mantel–Cox) test. Three biological replicates were conducted and are represented as mean \pm standard deviation ($n = 3$). Significant differences are denoted by * $p < 0.05$, ** $p < 0.01$, and *** $p < 0.001$, respectively.

3. Discussion

In this study, demethylcisterol A₃, along with five other compounds, was initially isolated from *P. sacchari*. As an incisterol-type steroid, demethylcisterol A₃ has been identified in various fungi, possibly representing a common metabolite in fungal processes [28–30]. Notably, demethylcisterol A₃ exhibits significant anti-tumor and anti-inflammatory effects [31,32]. Studies have demonstrated that the rate of inhibition exhibited by demethylcisterol A₃ towards *Helicobacter pylori* is 11% greater than that of 100 μ M quercetin [33]. Despite its recognized therapeutic potential, there has been limited research on its QS inhibitory effect against pathogens. Therefore, this study pioneers the investigation of demethylcisterol A₃'s impact on QS, biofilm formation, and virulence factors in *B. cereus*.

At the MIC, *B. cereus* growth was inhibited, but at sub-MICs, there was no significant effect (Figure 3). *B. cereus* biofilms contribute to equipment adhesion, increased resistance, and toxicity [34]. Following demethylcisterol A₃ treatment, biofilm formation was significantly inhibited, decreasing production by 50.2% at 3.12 μ g/mL. Our research is consistent with that pertaining to Siphonocholin, which can effectively inhibit biofilm formation at 1/2 MIC [35]. At the same time, diallyl disulfide can also inhibit the biofilm formation of *B. cereus* at 1/2 MIC [36]. The downregulation of *rpoN* and *comER*, important regulators of *B. cereus* biofilms, is associated with reduced biofilm production [37,38]. Additionally, the decrease in *tasA* expression directly correlates with a reduction in biofilm matrix protein synthesis [39].

B. cereus utilizes its swimming ability to navigate and reach the target host [36], and this mobility is intertwined with its biofilm formation [16]. Upon the addition of demethylcisterol A₃, both the swimming ability and the biofilm production of *B. cereus* decreased. Genes associated with flagella or mobility, including *rpoN*, *codY*, and *sinR* [38,40], showed significant downregulation after demethylcisterol A₃ treatment.

Proteases and hemolysin serve as virulence factors produced by *B. cereus*, aiding in immune system evasion [41]. Hemolysins induce red blood cell rupture, leading to hemolysis [42]. Following demethylcisterol A₃ treatment, *B. cereus* exhibited a significant reduction in protease and hemolysin production. In *B. cereus*, *nhe* represents non-hemolytic enterotoxin, *hbl* represents hemolysin BL, and *cytK* represents cytotoxin, regulated by *plcR* [42]. *papR* can produce PapR peptides to activate the PlcR protein [43]. Demethylcisterol A₃ reduced the mortality rate of *B. cereus* in the *G. mellonella* larval model from 75% to 12%. Furthermore, demethylcisterol A₃ diminished the transcription of the *nheA*, *hblD*, *cytK*, *plcR*, and *papR* genes in *B. cereus*. Therefore, demethylcisterol A₃ may mitigate the

production of virulence factors in *B. cereus*, weakening its pathogenicity by inhibiting the transcription of the *nheA*, *hblD*, *cytK*, *plcR*, and *papR* genes.

In the current study, cyclo-(L-Pro-L-Leu) was also extracted from *P. sacchari*. This cyclodipeptide was identified as a signaling molecule that facilitates communication between *B. cereus* and *Cronobacter sakazakii* [44]. It was already known whether or not it was a molecular signaling pathway in *B. cereus*; further research will be conducted to determine the above.

4. Materials and Methods

4.1. General

B. cereus (ATCC11778) was cultured using LB medium at 37 °C. Fresh *Laurencia* sp. was collected from the Nansha Islands area in the South China Sea (Figure S1), identified by Prof. X.L. Wang (Institute of Oceanology, CAS, China). The test compound was firstly dissolved in dimethyl sulfoxide (DMSO) to 1 mg/mL and sterilized using a filter membrane (0.22 µm) to obtain the stock solution. During all the experiments, an equal volume of DMSO was added as the negative control. The NMR was the Bruker Avance neo 400 (Bruker BioSpin AG, Ettlingen, Germany). The MS was ion trap time-of-flight mass spectrometry liquid chromatography-mass spectrometry (Shimadzu, Kyoto, Japan). All used chemicals in this work were analytical reagents.

4.2. Seaweed Sample Collection and Morphological Identification

The seaweed samples were collected by researcher Zhi-Kai Guo from the Institute of Biology, Chinese Academy of Tropical Agricultural Sciences, from the reef of Zhaoshu Island in the Xisha Xuande Islands. The algae species were identified by Professor Xu-Lei Wang from the Qingdao Institute of Oceanography, Chinese Academy of Sciences. The algal body was purplish red in appearance, with cylindrical branches—mostly forked or trifurcate branches, dense and clustered—with forked or threefold apical branchlets, and a concave apical center with trichonema. The tetrasporangium divides cruciform or conical. Identified as *Laurencia* sp. (Figure S1). Endophytes were extracted from algae. After placing fresh *Laurencia* sp. in a petri dish and disinfecting it three times with sterile water, it was rinsed with sterile water and alcohol for 30 seconds. It was then immersed in a 1% (*w/w*) NaClO solution for three minutes and then rinsed five times with sterile water. Once it was dried with filter paper, it was chopped into small segments. Mixed the small segments with sterile quartz sand. Then grinded the mixture in a sterile phosphate-buffered saline (PBS) environment. Diluted the grinding solution using a PBS gradient. A layer of 100 µL dilution solution (evenly distributed) was coated onto the culture plate containing PDA, Gause's Synthetic Agar No.1 (GSA) and LB. LB plate was cultured at 37 °C, while PDA and GSA plates were cultured at 28 °C. Colonies with different morphologies were selected for purification and preservation during the cultivation process.

4.3. Identification of QSI Active-Strain W2-F1

The QSI activities of the crude extract of ethyl acetate from the isolated strain were evaluated by using the indicator strain *Chromobacterium violaceum* CV026. Among these 7 isolates, W2-F1 showed the best QSI activity (Figure S2). The morphological characteristics of strain W2-F1 cultivated in PDA medium (Hope Bio, Qingdao, China) were examined [45]. Further, the genomic DNA was extracted and amplified using ITS primers (5'-TCCGTAGGTGGAACCTGGG-3' and 5'-TCTCCGCTTATTGCT-3') and the obtained sequence was aligned in the NCBI. Based on the sequence similarities, the phylogenetic tree was constructed by the neighbor-joining method with the 1000-bootstrap value using MEGA 7.0 software [46]. The W2-F1 strain was identified as *P. sacchari*.

4.4. Scale-Up Fermentation of QSI Active-Strain *P. sacchari* and Isolation, Purification, and Elucidation of Compounds under Bio-Guided Screenings

P. sacchari was activated on a PDA plate, then inoculated into a solid PDA medium containing 3% sea salt and cultured at 28 °C for 14 days. After the culture was completed, the mycelium was broken together with the culture medium. Absolute ethanol was added to the mixture and treated with ultrasonic for 12 h and then filtered, repeated three times. The ethanol in the filtrate was removed by evaporation under reduced pressure. The residual liquid was extracted three times by equal ethyl acetate (EtOAc) and concentrated under reduced pressure to give a crude extract (110.1 g), which was subjected to column chromatography (CC) over a silica gel (100–200 mesh) eluted with a gradient of CH₂Cl₂/MeOH (100:0–0:100) to obtain fractions (R1–R11). The fraction R4 (5.26 g) showing QSI activity was further submitted to silica gel (200–300 mesh) column chromatography (CC) and eluted with a gradient system of petroleum ether/CH₂Cl₂ (20:1–1:1) and CH₂Cl₂/MeOH (100:1–10:1) to obtain twenty-two subfractions (R4–1–22). Fraction R4–9 (0.24 g) showing QSI activity was purified by reversed-phase C₁₈ CC and semi-preparation HPLC equipped with a preparative column (5 µm, 21.2 × 250mm; Beijing, China) to obtain compounds 1 and 2 (eluting conditions: 100% MeOH, flow rate = 8 mL/min; yields: 4.8 and 8.7 mg). QSI-active R4–18 were eluted by silica gel column chromatography and semi-preparation HPLC to obtain compound 3 (eluting conditions: 90% MeOH, flow rate = 8 mL/min; yield: 3.2 mg) and R4–18–6. Compound 4 (yield: 10.8 mg) was obtained from R4–18–6 with a 60% MeOH eluting solution and a flow rate of 8 mL/min. Compounds 5 and 6 (yields: 7.4 and 7.5 mg) were obtained from R4–18–6 with a 50% MeOH elution solution and flow rate of 6 mL/min.

4.5. MIC of Demethylincisterol A₃ against *B. cereus*

MIC of demethylincisterol A₃ was measured by using the double dilution method [35]. The seed solution of *B. cereus* that was cultured overnight was added to LB medium at a rate of 1% (v/v). The compounds were added and the mixture was diluted and incubated at 37 °C and 180 rpm for 24 h. DMSO was used as the negative control. Growth profiles were measured at 620 nm.

4.6. Growth Measurement of *B. cereus*

The planktonic cell growth measurement was performed by the reported methods, with some modifications [47]. The *B. cereus* culture was inoculated into LB medium at a ratio of 1% (v/v). Demethylincisterol A₃ was then added to achieve final concentrations of 3.12, 1.56, and 0.78 µg/mL. After 24 hours of cultivation at 37 °C and 180 rpm, OD₆₂₀ was measured (Biotech Epoch 2, Santa Clara, CA, USA).

4.7. The Effects of Biofilm Formation

The biofilm formation assays were conducted following established procedures with slight modifications, as outlined in the report by [48]. *B. cereus* cultures that had been grown overnight were introduced into LB medium at a 1% (v/v) ratio, and demethylincisterol A₃ was added. A 200 µL aliquot of this mixed culture was then transferred to a 96-well polystyrene microtiter plate. The final concentrations of demethylincisterol A₃ in the wells were 3.12, 1.56, and 0.78 µg/mL. The plate was then incubated at 37 °C for 24 h. After this period, the culture medium was carefully removed and the wells were washed three times with sterile PBS to eliminate planktonic cells. The remaining water in the wells was evaporated at 60 °C. The biofilms that had adhered to the bottom of the wells were fixed with cool methanol for 15 min. The liquid was then removed and the plate was dried again at 60 °C. Each well was stained with 200 µL of a 0.05% (w/v) crystal violet solution. After 10 min staining, any excess crystal violet was removed and the wells were washed three times with PBS. Once the plate had dried at 60 °C, 200 µL of 95% (v/v) ethanol was added to each well and the plate was decolorized for 15 min on a shaker set at 37 °C and

180 rpm. A 150 μ L sample of the decolorizing solution was then taken from each well and the absorbance was measured at 570 nm.

SEM measurement: The coating was fixed on the glass slide with 2.5% (*v/v*) glutaraldehyde for 12 h. After fixation, it was washed at once with ultrapure water and then gradient dehydration was performed with 50%, 60%, 70%, 80%, 90%, and 100% (*v/v*) ethanol in sequence. After drying, it was sprayed gold and observed under a SEMn microscope.

4.8. Swimming Motility Assay

The swimming motility assay was evaluated by established protocols and reports, as per the study by [46]. Swimming medium (10 g/L peptone, 5 g/L NaCl, 3 g/L agar) was added to demethylcisterol A₃ to the final concentrations of 3.12, 1.56, and 0.78 μ g/mL, respectively. It was mixed well and poured evenly into a petri dish. Sterile water served as a negative control. After solidification, 2 μ L of *B. cereus* bacterial solution was inoculated in the center of the swimming medium. The migration diameter was recorded after 24 h of cultivation at 37 °C.

4.9. Measurement of Protease Production

Protease activities were measured by reported methods, with some modifications [49]. *B. cereus* cultures that had been grown overnight were introduced into LB medium at a 1% (*v/v*) ratio, and demethylcisterol A₃ was added. The final concentrations of demethylergosterol A₃ were 3.12, 1.56, and 0.78 μ g/mL, respectively. The solution was incubated at 37 °C and 180 rpm for 24 h. The fermentation broth was centrifuged (8000 \times *g*, 4 °C, 15 min) to collect the supernatant. The supernatant was filtered through a 0.22 μ m membrane. Skim milk agar was prepared (1/4-strength LB broth with 4% (*w/v*) skim milk and 1.5% (*w/v*) agar). Added 50 μ L of supernatant to the wells of a skim milk agar plate and incubated at 37 °C for 24 h. The protease activity was assessed by examining the clear zone on the skim milk agar plates.

4.10. Measurement of Hemolytic Activities

Hemolytic activities were measured by reported methods, with some modifications [50]. Hemolysis experiments were performed using a trypticase soy sheep blood agar plate (Huankai Microbial, Guangzhou, China). The supernatant was prepared according to the previous method. Then, 50 μ L of cultured supernatant was added after drilling, incubated at 37 °C for 24 h, and the size of the hemolytic halo was observed.

4.11. Quantitative Real-Time PCR

Quantitative real-time PCR (RT-qPCR) was performed according to reported methods, with minor modifications [48]. The bacterial solution cultured overnight was diluted to a 0.5 Michaelis turbidimetric unit with sterile LB broth. Overnight cultured *B. cereus* was added in a 1% (*v/v*) ratio to LB medium. The experimental group was supplemented with demethylcisterol A₃ to make its concentration 3.12 μ g/mL, and the same volume of DMSO was used as the negative control group. The solution was incubated at 37 °C and 180 rpm for 24 h. The fermentation broth was centrifuged (8000 \times *g*, 4 °C, 15 min) to collect cells and washed thrice with diethylpyrocarbonate (DEPC)-treated water. The total RNA of *B. cereus* was extracted using an Eastern[®] Super Total RNA Extraction Kit (Promega, Beijing, China) and transformed into cDNA by a Reverse Transcription Kit (Biosharp, Beijing, China). The real-time PCR reaction was performed using a TB Green[®] Premix Ex Taq[™] II FAST qPCR Mix (TaKaRa, Dalian, China) with a Bio-Rad CFX Connect System (Bio-Rad, Hercules, CA, USA). The primers used for real-time PCR are listed in Table 1. Gene 16S rRNA was used as an internal control [36].

Table 1. PCR primers for RT-qPCR.

Primer	Sequence (5'-3')
16S rRNA_F	GGAGGAAGGTGGGGATGAC
16S rRNA_R	ATGGTGTGACGGGCGGTGTG
sinR_F	AGCGAGCGCCGATATGATAG
sinR_R	TCGAGCGCATTTCGTAACCAT
tasA_F	ACTCGCCACATGGAAACACA
tasA_R	ACGATTTGTTTCGTTTTCTTCGT
papR_F	TGTACCTCTTGATCACTGTGAGA
papR_R	AACGTTAGCAATGGCATGGG
cytK_F	CGATGACCCAAGCGCTGATA
ctyK_R	GTTGCACTAGCACCAGGGAT
rpoN_F	CACTTGAACGAGCTTTCGCC
rpoN_R	GGGGCCGTAATATTCAGGA
hblD_F	GGTCCAGATGGGAAAGGTGG
hblD_R	AAGTTGTGGGATCGTTGCCT
comER_F	CAAGTTGCGGTCCTGCTTTC
comER_R	AATTTCCCCATCCCCACGAC
codY_F	CCACGACGGCTAACTACGAA
codY_R	GCGTTATTACAGAGCGCAGC
plcR_F	GGGTGATGCGGGGATTAACA
plcR_R	GGCTCACTTCCGATTGGTGA
nheA_F	TCTTGCAACAGCCAGACATT
nheA_R	CTCTCGCACATTTCGCCTTTG

4.12. Evaluating the Inhibitory Effect of Demethylcisterol A₃ in a *G. mellonella* Model

A *G. mellonella* larval model was used to evaluate the toxic inhibitory effect of demethylcisterol A₃ on *B. cereus* [51]. The supernatant was prepared as described above. The larvae were randomly divided into 15 groups ($n = 10$ per group) and 5 μ L of supernatant was injected into the posterior part of the left abdominal foot. Then, the larvae were cultured at room temperature for 72 h, and their growth was recorded every 12 h. PBS served as a blank control.

4.13. Statistical Analysis

Unless otherwise stated, all experiments described were performed in triplicate independently. The data shown in the figures are the mean \pm standard deviation (\pm SD) of the replicates. Statistical differences were determined using one-way ANOVA or *t*-test using GraphPad Prism 8, where $p < 0.05$ was considered statistically significant.

5. Conclusions

Demethylcisterol A₃ exhibits significant inhibitory effects on *B. cereus*, encompassing reduced biofilm formation, diminished bacterial mobility, and lowered production of virulence factors. This multifaceted impact has the potential to attenuate the pathogenicity of *B. cereus*. Based on these results, it can be inferred that demethylcisterol A₃ exhibits potential as a valuable compound in the development of novel antibacterial therapies.

Supplementary Materials: The following supporting information can be downloaded at <https://www.mdpi.com/article/10.3390/md22040161/s1>: Figure S1: *Laurencia* sp. was collected from the Nansha Islands area in the South China Sea; Figure S2: Evaluated QSI activities using the indicator strain of *Chromobacterium violaceum* CV026; Figure S3–S8: ¹H, ¹³C NMR, and HRMS data of compounds 1–6; Figure S9: Sequence comparison results of strain W2-F1; Figure S10–S13: Preparation spectrum of compounds 1–6; Table S1: The chemical shifts of each hydrogen-bearing chiral carbon.

Author Contributions: Conceptualization, S.-L.X.; data curation, S.-L.X. and K.-Z.X.; formal analysis, S.-L.X. and K.-Z.X.; funding acquisition, A.-Q.J.; investigation, S.-L.X.; methodology, S.-L.X. and L.-J.Y.; project administration, A.-Q.J.; resources, A.-Q.J.; software, S.-L.X. and L.-J.Y.; supervision, A.-Q.J.; writing—original draft, S.-L.X., K.-Z.X. and L.-J.Y.; writing—review and editing, A.-Q.J. All authors have read and agreed to the published version of the manuscript.

Funding: This research was funded by the Hainan Province Science and Technology Special Fund (ZDYF2024SHFZ103), the National Natural Science Foundation of China (82160664), and Innovative Research Projects for Postgraduates in Hainan Province (Qhyb2021-38, Qhyb2022-46).

Institutional Review Board Statement: Not applicable.

Data Availability Statement: The data presented in this study are available from the corresponding author upon request.

Acknowledgments: We thank the Hainan University for its support.

Conflicts of Interest: The authors declare no conflicts of interest.

References

- Pagarete, A.; Ramos, A.S.; Puntervoll, P.; Allen, M.J.; Verdelho, V. Antiviral potential of slgal metabolites—A comprehensive review. *Mar. Drugs* **2021**, *19*, 94. [[CrossRef](#)] [[PubMed](#)]
- Nagamalla, L.; Shanmukha Kumar, J.V.; Sanjay, C.; Alsamhan, A.M.; Shaik, M.R. In-silico study of seaweed secondary metabolites as AXL kinase inhibitors. *Saudi J. Biol. Sci.* **2022**, *29*, 689–701. [[CrossRef](#)] [[PubMed](#)]
- Vairagkar, U.; Mirza, Y. Antagonistic activity of antimicrobial metabolites produced from seaweed-associated *Bacillus amyloliquefaciens* MTCC 10456 against *Malassezia* spp. *Probiotics Antimicrob. Proteins* **2021**, *13*, 1228–1237. [[CrossRef](#)] [[PubMed](#)]
- Catarino, M.D.; Silva-Reis, R.; Chouh, A.; Silva, S.; Braga, S.S.; Silva, A.M.S.; Cardoso, S.M. Applications of antioxidant secondary metabolites of *Sargassum* spp. *Mar. Drugs* **2023**, *21*, 172. [[CrossRef](#)]
- Digra, S.; Nonzom, S. An insight into endophytic antimicrobial compounds: An updated analysis. *Plant Biotechnol. Rep.* **2023**, *17*, 427–457. [[CrossRef](#)] [[PubMed](#)]
- Stierle, A.; Strobel, G.; Stierle, D. Taxol and taxane production by *Taxomyces andreanae*, an endophytic fungus of Pacific yew. *Science* **1993**, *260*, 214–216. [[CrossRef](#)] [[PubMed](#)]
- Nishad, J.H.; Singh, A.; Gautam, V.S.; Kumari, P.; Kumar, J.; Yadav, M.; Kharwar, R.N. Bioactive potential evaluation and purification of compounds from an endophytic fungus *Diaporthe longicolla*, a resident of *Saraca asoca* (Roxb.) Willd. *Arch. Microbiol.* **2021**, *203*, 4179–4188. [[CrossRef](#)] [[PubMed](#)]
- Gautam, V.S.; Singh, A.; Kumari, P.; Nishad, J.H.; Kumar, J.; Yadav, M.; Bharti, R.; Prajapati, P.; Kharwar, R.N. Phenolic and flavonoid contents and antioxidant activity of an endophytic fungus *Nigrospora sphaerica* (EHL2), inhabiting the medicinal plant *Euphorbia hirta* (dudhi) L. *Arch. Microbiol.* **2022**, *204*, 140. [[CrossRef](#)]
- Xu, Z.; Xiong, B.; Xu, J. Chemical investigation of secondary metabolites produced by mangrove endophytic fungus *Phyllosticta capitalensis*. *Nat. Prod. Res.* **2021**, *35*, 1561–1565. [[CrossRef](#)]
- Singh, V.K.; Kumar, A. Secondary metabolites from endophytic fungi: Production, methods of analysis, and diverse pharmaceutical potential. *Symbiosis* **2023**, *90*, 111–125. [[CrossRef](#)]
- Akinpelu, D.A.; Aiyegoro, O.A.; Akinpelu, O.F.; Okoh, A.I. Stem bark extract and fraction of *Persea americana* (Mill.) exhibits bactericidal activities against strains of *Bacillus cereus* associated with food poisoning. *Molecules* **2015**, *20*, 416–429. [[CrossRef](#)] [[PubMed](#)]
- Eglezos, S.; Huang, B.; Dykes, G.A.; Fegan, N. The prevalence and concentration of *Bacillus cereus* in retail food products in Brisbane, Australia. *Foodborne Pathog. Dis.* **2010**, *7*, 867–870. [[CrossRef](#)] [[PubMed](#)]
- Leong, S.S.; Korel, F.; King, J.H. *Bacillus cereus*: A review of “fried rice syndrome” causative agents. *Microb. Pathog.* **2023**, *185*, 106418. [[CrossRef](#)] [[PubMed](#)]
- Lin, Y.; Briandet, R.; Kovács, Á.T. *Bacillus cereus* sensu lato biofilm formation and its ecological importance. *Biofilm* **2022**, *4*, 100070. [[CrossRef](#)] [[PubMed](#)]
- Huang, Y.; Flint, S.H.; Palmer, J.S. *Bacillus cereus* spores and toxins—the potential role of biofilms. *Food Microbiol.* **2020**, *90*, 103493. [[CrossRef](#)] [[PubMed](#)]
- Zhao, L.; Duan, F.; Gong, M.; Tian, X.; Guo, Y.; Jia, L.; Deng, S. (+)-Terpinen-4-ol Inhibits *Bacillus cereus* biofilm formation by upregulating the interspecies quorum sensing signals diketopiperazines and diffusing signaling factors. *J. Agric. Food Chem.* **2021**, *69*, 3496–3510. [[CrossRef](#)] [[PubMed](#)]
- Gorgan, M.; Vanunu Ofri, S.; Engler, E.R.; Yehuda, A.; Hutnick, E.; Hayouka, Z.; Bertucci, M.A. The importance of the PapR7 C-terminus and amide protons in mediating quorum sensing in *Bacillus cereus*. *Res. Microbiol.* **2023**, *174*, 104139. [[CrossRef](#)] [[PubMed](#)]

18. Amagata, T.; Tanaka, M.; Yamada, T.; Doi, M.; Minoura, K.; Ohishi, H.; Yamori, T.; Numata, A. Variation in cytostatic constituents of a sponge-derived *Gymnascella dankaliensis* by manipulating the carbon source. *J. Nat. Prod.* **2007**, *70*, 1731–1740. [[CrossRef](#)] [[PubMed](#)]
19. Mansoor, T.A.; Hong, J.; Lee, C.-O.; Bae, S.-J.; Im, K.S.; Jung, J.H. Cytotoxic sterol derivatives from a marine sponge *Homaxinella* sp. *J. Nat. Prod.* **2005**, *68*, 331–336. [[CrossRef](#)]
20. Yajima, A.; Kagohara, Y.; Shikai, K.; Katsuta, R.; Nukada, T. Synthesis of two osteoclast-forming suppressors, demethylincisterol A₃ and chaxine A. *Tetrahedron* **2012**, *68*, 1729–1735. [[CrossRef](#)]
21. Yang, X.-L.; Zhang, S.; Hu, Q.-B.; Luo, D.-Q.; Zhang, Y. Phthalide derivatives with antifungal activities against the plant pathogens isolated from the liquid culture of *Pestalotiopsis photiniae*. *J. Antibiot.* **2011**, *64*, 723–727. [[CrossRef](#)]
22. Mehnaz, S.; Saleem, R.S.Z.; Yameen, B.; Pianet, I.; Schnakenburg, G.; Pietraszkiewicz, H.; Valeriote, F.; Josten, M.; Sahl, H.-G.; Franzblau, S.G.; et al. Lahorenoic acids A–C, ortho-dialkyl-substituted aromatic acids from the biocontrol strain *Pseudomonas aurantiaca* PB-St2. *J. Nat. Prod.* **2013**, *76*, 135–141. [[CrossRef](#)]
23. Campbell, J.; Lin, Q.; Geske, G.D.; Blackwell, H.E. New and Unexpected Insights into the Modulation of LuxR-Type Quorum Sensing by Cyclic Dipeptides. *ACS Chem. Bio.* **2009**, *4*, 1051–1059. [[CrossRef](#)]
24. Fdhila, F.; Vázquez, V.; Sánchez, J.L.; Riguera, R. DD-Diketopiperazines: Antibiotics Active against *Vibrio anguillarum* Isolated from Marine Bacteria Associated with Cultures of *Pecten maximus*. *J. Nat. Prod.* **2003**, *66*, 1299–1301. [[CrossRef](#)]
25. Song, S.; Fu, S.; Sun, X.; Li, P.; Wu, J.E.; Dong, T.; He, F.; Deng, Y. Identification of cyclic dipeptides from *Escherichia coli* as new antimicrobial agents against *Ralstonia solanacearum*. *Molecules* **2018**, *23*, 214. [[CrossRef](#)]
26. Yang, B.; Dong, J.; Zhou, X.; Yang, X.; Lee, K.J.; Wang, L.; Zhang, S.; Liu, Y. Proline-containing dipeptides from a marine sponge of a *Callyspongia* Species. *Helv. Chim. Acta* **2009**, *92*, 1112–1117. [[CrossRef](#)]
27. Han, Y.; Li, Y.Y.; Shen, Y.; Li, J.; Li, W.J.; Shen, Y.M. Oxoprothracarin, a novel pyrrolo[1,4]benzodiazepine antibiotic from marine *Streptomyces* sp. M10946. *Drug Discov. Ther.* **2013**, *7*, 243–247. [[CrossRef](#)] [[PubMed](#)]
28. Yang, X.; Wu, P.; Xue, J.; Li, H.; Wei, X. Seco-pimarane diterpenoids and androstane steroids from an endophytic *Nodulisporium* fungus derived from *Cyclosorus parasiticus*. *Phytochemistry* **2023**, *210*, 113679. [[CrossRef](#)]
29. Li, D.X.; Cheng, X.; Ma, F.P.; Chen, J.Y.; Chen, Y.P.; Zhao, X.S.; Luo, Q. Identification of metabolites from edible mushroom *Morchella sextelata* and their biological evaluation. *Nat. Prod. Res.* **2023**, *37*, 1774–1781. [[CrossRef](#)] [[PubMed](#)]
30. Jiang, C.; Ji, J.; Li, P.; Liu, W.; Yu, H.; Yang, X.; Xu, L.; Guo, L.; Fan, Y. New lanostane-type triterpenoids with proangiogenic activity from the fruiting body of *Ganoderma applanatum*. *Nat. Prod. Res.* **2022**, *36*, 1529–1535. [[CrossRef](#)]
31. Su, J.-C.; Pan, Q.; Xu, X.; Wei, X.; Lei, X.; Zhang, P. Structurally diverse steroids from an endophyte of *Aspergillus tennesseensis* 1022LEF attenuates LPS-induced inflammatory response through the cholinergic anti-inflammatory pathway. *Chem.-Biol. Interact.* **2022**, *362*, 109998. [[CrossRef](#)] [[PubMed](#)]
32. Liu, Y.; Fu, H.; Zuo, L. Synergistic cytotoxicity effect of 5-Fluorouracil and SHP2 Inhibitor demethylincisterol A₃ on cervical cancer cell. *Anti-Cancer Agents Med. Chem.* **2022**, *22*, 1313–1319. [[CrossRef](#)] [[PubMed](#)]
33. Na, M.W.; Lee, E.; Kang, D.-M.; Jeong, S.Y.; Ryoo, R.; Kim, C.-Y.; Ahn, M.-J.; Kang, K.B.; Kim, K.H. Identification of antibacterial sterols from Korean wild mushroom *Daedaleopsis confragosa* via bioactivity- and LC-MS/MS profile-guided fractionation. *Molecules* **2022**, *27*, 1865. [[CrossRef](#)] [[PubMed](#)]
34. Huang, Y.; Flint, S.H.; Loo, T.S.; Palmer, J.S. Emetic toxin production of *Bacillus cereus* in a biofilm. *LWT-Food Sci. Technol.* **2022**, *154*, 112840. [[CrossRef](#)]
35. Alam, P.; Alqahtani, A.S.; Mabood Husain, F.; Tabish Rehman, M.; Alajmi, M.F.; Noman, O.M.; El Gamal, A.A.; Al-Massarani, S.M.; Shavez Khan, M. Siphonocholin isolated from red sea sponge *Siphonochalina siphonella* attenuates quorum sensing controlled virulence and biofilm formation. *Saudi Pharm. J.* **2020**, *28*, 1383–1391. [[CrossRef](#)] [[PubMed](#)]
36. Jin, Z.; Li, L.; Zheng, Y.; An, P. Diallyl disulfide, the antibacterial component of garlic essential oil, inhibits the toxicity of *Bacillus cereus* ATCC 14579 at sub-inhibitory concentrations. *Food Control* **2021**, *126*, 108090. [[CrossRef](#)]
37. Hayrapetyan, H.; Tempelaars, M.; Nierop Groot, M.; Abee, T. *Bacillus cereus* ATCC 14579 RpoN (Sigma 54) Is a pleiotropic regulator of growth, carbohydrate metabolism, motility, biofilm formation and toxin production. *PLoS ONE* **2015**, *10*, e0134872. [[CrossRef](#)] [[PubMed](#)]
38. Yan, F.; Yu, Y.; Wang, L.; Luo, Y.; Guo, J.-h.; Chai, Y. The *comER* gene plays an Important role in biofilm formation and sporulation in both *Bacillus subtilis* and *Bacillus cereus*. *Front. Microbiol.* **2016**, *7*, 1025. [[CrossRef](#)] [[PubMed](#)]
39. Caro-Astorga, J.; Pérez-García, A.; de Vicente, A.; Romero, D. A genomic region involved in the formation of adhesin fibers in *Bacillus cereus* biofilms. *Front. Microbiol.* **2015**, *5*, 745. [[CrossRef](#)]
40. Coburn, P.S.; Miller, F.C.; Enty, M.A.; Land, C.; LaGrow, A.L.; Mursalin, M.H.; Callegan, M.C. The *Bacillus virulome* in endophthalmitis. *Microbiology* **2021**, *167*, 001057. [[CrossRef](#)]
41. Dietrich, R.; Jessberger, N.; Ehling-Schulz, M.; Märtlbauer, E.; Granum, P.E. The food poisoning toxins of *Bacillus cereus*. *Toxins* **2021**, *13*, 98. [[CrossRef](#)]
42. Enosi Tuipulotu, D.; Mathur, A.; Ngo, C.; Man, S.M. *Bacillus cereus*: Epidemiology, virulence factors, and host-pathogen interactions. *Trends Microbiol.* **2021**, *29*, 458–471. [[CrossRef](#)]
43. Huillet, E.; Bridoux, L.; Barboza, I.; Lemy, C.; André-Leroux, G.; Lereclus, D. The signaling peptide PapR is required for the activity of the quorum-sensor PlcRa in *Bacillus thuringiensis*. *Microbiology* **2020**, *166*, 398–410. [[CrossRef](#)]

44. Bofinger, M.R.; de Sousa, L.S.; Fontes, J.E.N.; Marsaioli, A.J. Diketopiperazines as cross-communication quorum-sensing signals between *Cronobacter sakazakii* and *Bacillus cereus*. *ACS Omega* **2017**, *2*, 1003–1008. [[CrossRef](#)] [[PubMed](#)]
45. Shafique, S.; Javed, A.; Shafique, S.; Hussain, A.; Rafique, R.; Mubarak, A. Isolation and identification of *Pithomyces sacchari* as a leaf spot pathogen of *Helianthus annuus* from Pakistan. *Sci. Rep.* **2022**, *12*, 22033. [[CrossRef](#)]
46. Zeng, Y.X.; Liu, J.S.; Wang, Y.J.; Tang, S.; Wang, D.Y.; Deng, S.M.; Jia, A.Q. Actinomycin D: A novel *Pseudomonas aeruginosa* quorum sensing inhibitor from the endophyte *Streptomyces cyaneochromogenes* RC1. *World J. Microbiol. Biotechnol.* **2022**, *38*, 170. [[CrossRef](#)] [[PubMed](#)]
47. Inaba, M.; Matsuda, N.; Banno, H.; Jin, W.; Wachino, J.-i.; Yamada, K.; Kimura, K.; Arakawa, Y. In vitro reduction of antibacterial activity of tigecycline against multidrug-resistant *Acinetobacter baumannii* with host stress hormone norepinephrine. *Int. J. Antimicrob. Agents* **2016**, *48*, 680–689. [[CrossRef](#)] [[PubMed](#)]
48. Xu, K.-Z.; Xiang, S.-L.; Wang, Y.-J.; Wang, B.; Jia, A.-Q. Methyl gallate isolated from partridge tea (*Mallotus oblongifolius* (Miq.) Müll.Arg.) inhibits the biofilms and virulence factors of *Burkholderia thailandensis*. *J. Ethnopharmacol.* **2024**, *320*, 117422. [[CrossRef](#)]
49. Chu, W.; Zhou, S.; Jiang, Y.; Zhu, W.; Zhuang, X.; Fu, J. Effect of traditional Chinese herbal medicine with anti-quorum sensing activity on *Pseudomonas aeruginosa*. *Evid.-Based Complement. Altern. Med.* **2013**, *2013*, 648257. [[CrossRef](#)]
50. Zhao, Y.; Chen, C.; Gu, H.-j.; Zhang, J.; Sun, L. Characterization of the genome feature and toxic capacity of a *Bacillus wiedmannii* isolate from the hydrothermal field in Okinawa Trough. *Front. Cell. Infect. Microbiol.* **2019**, *9*, 370. [[CrossRef](#)]
51. Yin, L.; Wang, Y.; Xiang, S.; Xu, K.; Wang, B.; Jia, A.-Q. Tyramine, one quorum sensing inhibitor, reduces pathogenicity and restores tetracycline susceptibility in *Burkholderia cenocepacia*. *Biochem. Pharmacol.* **2023**, *218*, 115906. [[CrossRef](#)] [[PubMed](#)]

Disclaimer/Publisher's Note: The statements, opinions and data contained in all publications are solely those of the individual author(s) and contributor(s) and not of MDPI and/or the editor(s). MDPI and/or the editor(s) disclaim responsibility for any injury to people or property resulting from any ideas, methods, instructions or products referred to in the content.